Plant Physiology Preview. Published on July 21, 2017, as DOI:10.1104/pp.17.00535

Running title: Linking auxin with photosynthesis

Title: **Linking auxin with photosynthetic rate via leaf venation**

Author Affiliation:

Scott A. M. McAdam[1], Morgane P. Eléouët[2], Melanie Best[1], Timothy J. Brodribb[1], Madeline Carins Murphy[1], Sam D. Cook[1], Marion Dalmais[3], Theodore Dimitriou[1], Ariane Gélinas-Marion[1], Warwick M. Gill[5], Matthew Hegarty[2], Julie M. I. Hofer[2], Mary Maconochie[1], Erin L. McAdam[1], Peter McGuiness[1], David S. Nichols[4], John J. Ross[1], Frances C. Sussmilch[1] and Shelley Urquhart[1]

[1] School of Biological Sciences, University of Tasmania, Hobart, TAS, 7001, AUSTRALIA

[2] Institute of Biological, Environmental and Rural Sciences, Aberystwyth University, Aberystwyth SY23 3EE, UNITED KINGDOM

[3] Institue of Plant Sciences Paris Saclay IPS2, CNRS, INRA, Université Paris-Sud, Université Evry, Université Paris-Saclay, Baitment 630, 91405 Orsay, FRANCE

[4] Central Science Laboratory, University of Tasmania, Hobart, TAS, 7001, AUSTRALIA

[5] Tasmanian Institute of Agriculture and School of Land and Food, University of Tasmania, Hobart, TAS, 7001, AUSTRALIA

Corresponding author:

Scott McAdam
School of Biological Sciences
University of Tasmania
Private Bag 55, Hobart, TAS, 7001
AUSTRALIA

Keywords: Auxin, photosynthesis, venation, vein density, leaf hydraulic conductivity

Author contributions: S.A.M.M. developed the research plans for and supervised measurements of anatomy, gas exchange and hydraulics and wrote the manuscript with contributions from J.M.I.H. and M.P.E. who designed the research plans for molecular and phenotypic characterisation of mutant alleles; A.G-M. performed auxin quantifications and auxin activity analyses writing relevant sections; S.D.C. prepared phylogenetic analyses, writing relevant sections; F.C.S. molecularly characterised a mutant allele and wrote relevant sections; E.L.M. acquired lines for auxin activity

Downloaded from on August 3, 2017 - Published by www.plantphysiol.org
Copyright © 2017 American Society of Plant Biologists. All rights reserved.
Copyright 2017 by the American Society of Plant Biologists

analyses; M.B., T.D., M.M., S.U. and M.C.M. collected anatomical and physiological data; P.M. designed specialised software for anatomical analyses; M.D. developed a mutant allele; D.S.N. assisted in the quantification of auxin; W.M.G. undertook resin imbedding; M.H. supervised and assisted in the characaterisation of a mutant allele; T.J.B. assisted in experimental design; and J.J.R first observed the *pss* allele and complemented the writing.

Funding information: The TILLING platform was supported by the ERC Advanced Grant SEXYPARTH (MD). This work was supported by the Australian Research Council (grants DE140100946 (SAMM), DP140100666 (TJB) and DP130103357 (JJR)).

One-Sentence summary: Auxin influences maximum leaf photosynthetic rate through leaf venation and thus water transport capacity.

Abstract

Land plants lose vast quantities of water to the atmosphere during photosynthetic gas exchange. In angiosperms a complex network of veins irrigates the leaf, and it is widely held that the density and placement of these veins determines maximum leaf hydraulic capacity and thus maximum photosynthetic rate. This theory is largely based on interspecific comparisons and has never been tested using vein mutants to examine the specific impact of leaf vein morphology on plant water relations. Here we characterise mutants at the *Crispoid* (*Crd*) locus in *Pisum sativum*, which have altered auxin homeostasis and activity in developing leaves, as well as reduced leaf vein density and aberrant placement of free-ending veinlets. This altered vein phenotype in *crd* mutant plants results in a significant reduction in leaf hydraulic conductance and leaf gas exchange. We find *Crispoid* to be a member of the *YUCCA* family of auxin biosynthetic genes. Our results link auxin biosynthesis with maximum photosynthetic rate through leaf venation, and substantiate the theory that an increase in the density of leaf veins coupled with their efficient placement can drive increases in leaf photosynthetic capacity.

Introduction

A central requirement for photosynthesis on land is the uptake of CO_2 from the atmosphere. In order to assimilate just one molecule of atmospheric CO_2, plants on average lose 150 molecules of water (Wong et al., 1979). To supply this high demand for water an internal transport system comprised of xylem conduits irrigates the leaf. Higher rates of photosynthesis (*A*) are linked to higher rates of transpiration, thus demanding greater efficiency in the transport and delivery of water to evaporating leaf tissue (Brodribb and Feild, 2000; Tyree and Zimmermann, 2002; Sack and Scoffoni, 2013). The xylem transports water efficiently through non-living tubular cells in the leaf,

Downloaded from on August 3, 2017 - Published by www.plantphysiol.org
Copyright © 2017 American Society of Plant Biologists. All rights reserved.

yet the last part of the pathway involves a significantly slower transfer through living mesophyll cells to the stomata. The length of this final non-xylem transfer has a major influence on the efficiency of the entire water transport system (Brodribb et al., 2007). Current theory posits that as hydraulic supply is essential for *A*, a reduction in the mean path-length for water flow through the mesophyll will increase leaf hydraulic conductance (K_{leaf}), which will increase stomatal conductance (g_s) and consequently theoretical maximum *A* (Sack and Frole, 2006; Brodribb et al., 2007; Brodribb et al., 2010; Scoffoni et al., 2011; Scoffoni et al., 2016).

A core body of literature has identified a number of adaptations that reduce the terminal path-length for water flow in the leaf and thus increase K_{leaf}. These adaptations range from increasing the density of the veins per unit area of leaf (Brodribb et al., 2007; Sack et al., 2013; Caringella et al., 2015), modifying leaf thickness and bundle sheath extensions (Sack et al., 2003; Zsögön et al., 2015) through to the formation of accessory transfusion tissue (Brodribb and Holbrook, 2005), and the formation and placement of free-ending veinlets (FEVs) within areoles (the small area of leaf mesophyll bound on all sides by veins) (Scoffoni et al., 2011; Fiorin et al., 2016). Of these adaptations, vein density has been a major focus due to the high plasticity of this trait both within species (Carins Murphy et al., 2012; Scoffoni et al., 2015) and across vascular plant taxa (Boyce et al., 2009). Using this variation in vein density, strong correlations have been established between the terminal path length for water flow through the mesophyll and maximum K_{leaf} (Sack and Frole, 2006; Brodribb et al., 2007; Brodribb et al., 2010; Sack et al., 2013; Scoffoni et al., 2016). These correlations are supported by single-gene vein density mutants in *Arabidopsis thaliana* and *Solanum lycopersicum* spanning a spectrum of vein modifications that influence K_{leaf} (Caringella et al., 2015; Zsögön et al., 2015).

The importance of K_{leaf} lies in its positive correlation with *A*. Selection for greater *A* and productivity is believed to have been the primary driver behind the > 10 fold increase in vein density that is observed in the fossil record over the past 400 million years, from the single-veined leaves of lycophytes to the highly complex, hierarchical networks of leaf veins in angiosperms (Brodribb et al., 2005; Boyce et al., 2009; Zhang et al., 2014). This increase in vein density is correlated with an equally substantial increase in maximum *A* across extant lineages that diverged during this major transition in leaf anatomy. Similar correlations between vein density, K_{leaf} and *A* can be observed within angiosperms (Brodribb and Feild, 2010; Carins Murphy et al., 2012; Scoffoni et al., 2015; Scoffoni et al., 2016).

However, this correlative evidence does not prove that changes in venation are responsible for changes in *A*, especially considering that stomatal and/or epidermal traits, which can also strongly

Downloaded from on August 3, 2017 - Published by www.plantphysiol.org
Copyright © 2017 American Society of Plant Biologists. All rights reserved.

94 influence maximum leaf gas exchange, are highly coordinated with vein density (Brodribb and Jordan,
95 2011; Carins Murphy et al., 2012; Carins Murphy et al., 2016). Here we use the powerful tool of
96 physiological genetics to address the relationships between venation, water transport and *A*. A
97 number of mutants, particularly those related to auxin biosynthesis or signalling, have either
98 reduced vein densities, aberrant vein topologies or defective vein formation (Tobeña-Santamaria et
99 al., 2002; Scarpella and Meijer, 2004; Cheng et al., 2006; Cheng et al., 2007; Verna et al., 2015).
100 Indeed, the auxin canalization theory, based on observations of a self-organising flux of auxin that
101 initiates a vascular cambium, effectively predicts the formation and development of leaf vein
102 networks (Sachs 1981; Lee et al., 2014; Rolland-Lagan and Prusinkiewicz, 2005). While the vein-
103 patterning mutant resource has been invaluable for studying both auxin biosynthesis and the role of
104 the auxin stream in leaf vascular formation, no study to date has examined whether these mutations
105 affect vein networks independently of changes in stomatal density or anatomy, and if so, whether
106 these vein defects influence K_{leaf}, maximum leaf gas exchange, and most importantly, *A*.

107 In this study we characterise mutations at the *Crispoid* (*Crd*) locus of *Pisum sativum* (Swiecicki, 1989;
108 Berdnikov et al., 2000). We show that *Crd* corresponds to the *PsYUC1* gene, a member of the *YUCCA*
109 gene family known to encode key auxin biosynthesis enzymes (Zhao et al., 2001; Mashiguchi et al.,
110 2011). We comprehensively describe aberrations in the vein morphology, topology, maximum leaf
111 gas exchange and K_{leaf} in the *crd-4* mutant. We use this mutant to test the hypothesis that maximum
112 *A* is determined by the distance water must travel through the mesophyll. We show that maximum *A*
113 is regulated by auxin through leaf venation.

114

Downloaded from on August 3, 2017 - Published by www.plantphysiol.org
Copyright © 2017 American Society of Plant Biologists. All rights reserved.

Results

crispoid *mutants carry lesions in the pea homologue of* AtYUC1/AtYUC4/PhFLOOZY

Homozygous recessive *crd* mutants are easily distinguished from wild-type (Swiecicki, 1989; Berdnikov et al., 2000) plants due to a noticeable reduction in vein density (Figure 1A and 1B; Supplementary Table S1). Two mutants with similar defective venation phenotypes were identified and shown to be additional alleles of the *Crd* locus by complementation testing (Supplementary Figure S1). The recessive mutant alleles were named *crd-1* (Swiecicki, 1989), *crd-2* (Berdnikov et al., 2000), *crd-3* (FN 1522/1) and *crd-4* (UTILLdb L905). In order to identify the gene affected in the *crd* mutants, we used a next generation RNA sequencing approach, focussing on the identification of any transcripts missing from the *crd-3* allele, as most lesions characterised so far from the JI 2822-derived fast-neutron mutant population have been large, gene-sized deletions (Domoney et al., 2013). We assembled a reference transcriptome from the corresponding wild-type line (WT-3) comprising 79,693 contigs (N50 = 1,191bp), and used this reference transcriptome to map reads from triplicate *crd-3* samples. We identified two contigs that showed significant differences in expression between the *crd-3* and WT-3 genotypes (FDR corrected p-value < 0.05). Only one contig, 435 bp in length, was expressed in WT-3 samples but showed complete absence of expression in *crd-3* mutant samples, consistent with a fast neutron-generated deletion. This contig corresponded to the entire last exon and portion of the 3' UTR of *PsYUC1*, a previously identified pea homologue of *AtYUC1*/*AtYUC4*/*PhFLOOZY*, encoding a 411 amino acid flavin-containing mono-oxygenase (FMO) protein (Tivendale et al., 2010).

In order to test whether *PsYUC1* corresponds to the *Crd* locus, the four known *crd* mutant alleles were characterised further. We identified a 425G>A SNP in the *crd-1* allele (Figure 1C), which would result in a 142G>D amino acid substitution within the ATG-containing motif 1 conserved between YUCCA proteins (Liu et al., 2012). A single 628G>A SNP was identified in the coding sequence of the *crd-2* allele, which is predicted to cause an intron 1 splicing defect (Figure 1C). Accordingly, PCR analysis of *crd-2* cDNA showed several transcripts of different sizes (Supplementary Figure S2). Sequencing confirmed that the largest of these transcripts contained the unspliced intron 1, which would encode a protein product with a frameshift at position 210 and premature termination after 244 amino acids (Supplementary Figure S3). A smaller mis-spliced *crd-2* transcript was found to contain 4 bp of intron 1, which would also result in a frameshift at position 210 and premature termination of the protein product after 262 amino acids. No portion of the *PsYUC1* gene could be amplified from *crd-3* genomic DNA template, using PCR primer pairs spanning the full length of the

Downloaded from on August 3, 2017 - Published by www.plantphysiol.org
Copyright © 2017 American Society of Plant Biologists. All rights reserved.

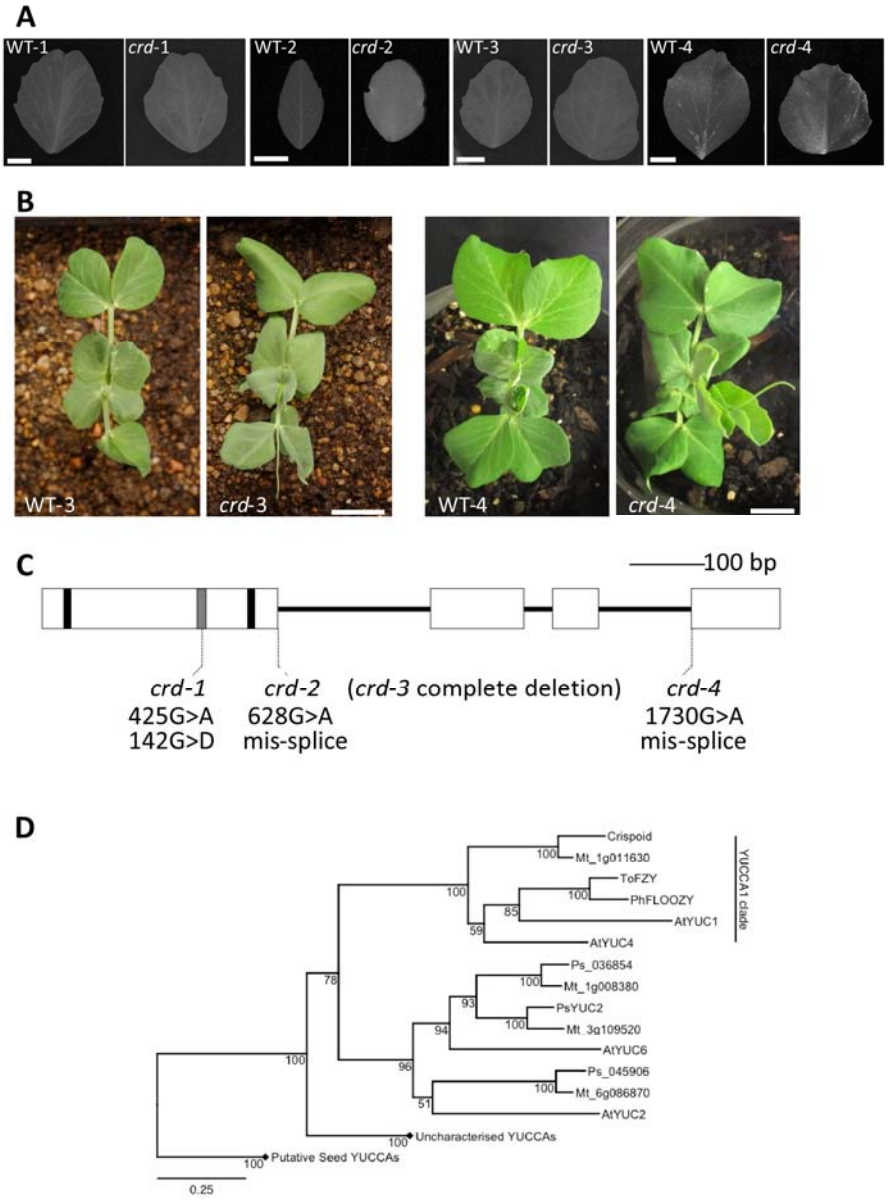

Figure 1. (A) Representative leaflets from node 6 taken from each *crd* mutant allele and respective wild-type. A 1 cm scale marker for each pair is shown in the wild-type image of each pairing. (B) Aerial view of seedlings of WT-3 and *crd-3* (left) and WT-4 and *crd-4* (right) showing node 4 leaves uppermost in each panel. A 2 cm scale marker for each pair of images is shown on the mutant image of each pairing. Similar images or comprehensive phenotypic details of *crd-1* and *crd-2* seedlings are provided by Swiecicki (1989) and Berdnikov et al. (2000), respectively. (C) Diagram of *Crd* gene showing regions encoding conserved motifs and the positions of crd mutations. Exons are shown as boxes, nucleotides encoding FAD- and NADPH-binding motifs are shown as black bars, ATG-containing motif 1 is shown as a grey bar. (D) Phylogenetic analysis of YUCCA protein sequences from *M. truncatula* (Mt), *P. sativum* (Ps) and *A. thaliana* (At), as well as ToFZY (*Solanum lycopersicum*), PhFLOOZY (*Petunia* x *hybrida*). Bootstrap values (from 1000 iterations) for this BIONJ tree are displayed adjacent to nodes and the scale bar indicates genetic distance (0.25 changes/amino acid). Diamonds indicate collapsed clades belonging to the putative, but uncharacterised seed YUCCA clades. Accession numbers for all genes are given in Supplementary Table S2.

147 gene, suggesting that *crd-3* is a null allele corresponding to complete deletion of *PsYUC1*

148 (Supplementary Figure S4). The *crd-4* allele was characterised as a 1730G>A SNP which would shift

149 the intron 3 splice acceptor site 1 bp downstream relative to WT-4. This would cause a frameshift at

Downloaded from on August 3, 2017 - Published by www.plantphysiol.org
Copyright © 2017 American Society of Plant Biologists. All rights reserved.

position 334 of the protein product, with 27 nonsense amino acids preceding premature termination of the protein.

Crd and *PsYUC1* co-segregated in an F_3 population of 96 individuals, which is consistent with these representing the same locus. Furthermore, genetic mapping located *PsYUC1* on pea LG II, at a position consistent with the *Crd* locus. On the basis of the strong evidence provided by this RNA-seq data, co-segregation analysis and the significant lesions characterised in four independent alleles, we concluded that the *Crd* locus corresponds to the *PsYUC1* gene. Phylogenetic analysis revealed that of the twelve *FMO* genes most closely related to *AtYUC1/AtYUC4/PhFLOOZY* identified in the *P. sativum* gene atlas (Alves-Carvalho et al., 2015), *Crd* is the only gene that groups with members of the *AtYUC1*/*AtYUC4/PhFLOOZY/SlFZY* clade (Figure 1D), indicating the *Crd* is the *P. sativum* orthologue. This conclusion is further supported by the finding that there is also only a single *Medicago truncatula* gene, Medtr1g011630, that groups within this clade present in the genome of *M. truncatula* (Figure 1D). *M. truncatula* is a sequenced legume closely related to *P. sativum* and their genomes are collinear in this region (Tayeh et al., 2015). Reciprocal BLASTn searches of the *M. truncatula* genome (v4) and pea transcriptome databases showed that *Crd* is most similar to Med1g011630; they likely represent an orthologous pair.

Altered vein topology in crispoid *mutants*

A common feature of all *crd* mutant alleles is a reduction in vein density at both a macroscopic and microscopic level (Figures 1A, 1B, 2A and 2B; Supplementary Table S1). Major vein density is reduced in the mutant alleles, with a significant reduction in the density of either or both secondary and tertiary orders of veins in mutants compared to WT leaves (Figure 1A; Supplementary Table S1). A more comprehensive microscopic examination of *crd-4* mutant leaves revealed a 20% reduction in minor vein density compared to WT-4 leaves (Figure 2C). This reduction is not associated with changes in stomatal density or stomatal size, with both of these traits being the same as in WT-4 plants (Figure 2D and E). The placement and development of FEVs in areoles was also severely altered in the *crd-4* mutant (Figure 3). In WT-4 plants the mean distance from the stomata to the nearest vein showed little variability across the spectrum of areole sizes. In contrast, and consistent with observations of lower vein density, *crd-4* mutants had a significantly greater mean distance from the stomata to the nearest vein compared to WT-4 across areole sizes (t-test, $P<0.001$), as well as a significantly greater variance in the mean distance from stomata to the nearest vein (F-test, $P<0.001$) (Figure 3). The development of FEVs was substantially reduced in *crd-4* mutant plants compared to WT-4 plants (Figure 3B and 3C), which in addition to a lower vein density contributed to the greater mean distance from stomata to the nearest vein. In WT-4 plants, only 60% of the

Downloaded from on August 3, 2017 - Published by www.plantphysiol.org
Copyright © 2017 American Society of Plant Biologists. All rights reserved.

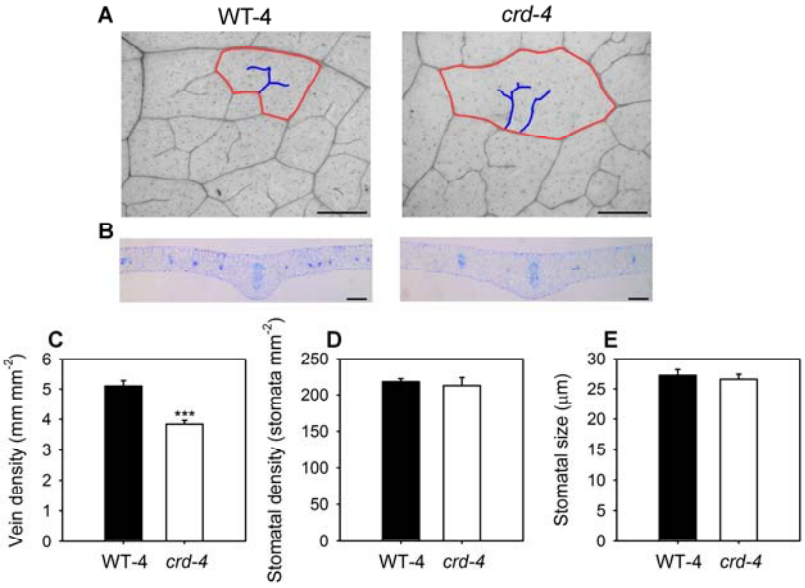

Figure 2. (A) A representative longitudinal image of leaf venation in WT-4 and *crd-4* leaves (scale bar = 200 µm, red lines outline an areole, blue lines highlight free ending veinlets within the areole). (B) A representative cross-sectional image of WT-4 and *crd-4* mutant leaves through the midrib (scale bar = 200 µm). (C) Mean vein density (n=7 leaves, ±SE), (D) stomatal density (n=7 leaves, ±SE) and (E) stomatal size (n=50 stomata, ±SE) in WT-4 and *crd-4* mutant plants. Asterisks denote significant difference in means (P<0.001).

smallest size class of areoles lacked FEVs, with all areoles larger than 0.15 mm^2 having these structures (Figure 3B). In *crd-4* plants, all areoles less than 0.15 mm^2 lacked FEVs and only areoles greater than 0.5 mm^2 consistently developed FEVs in this mutant (Figure 3C).

Leaf hydraulic capacity and gas exchange in crispoid *mutants*

Maximum K_{leaf} was reduced in *crd-4* mutant plants, being 30% lower than in WT-4 plants (Figure 4). Leaf gas exchange was also significantly reduced in the *crd-4* mutant plants compared to WT-4 plants at both high and low VPD (Figure 4). Leaf gas exchange parameters including A and g_s in WT-4 plants were double that of *crd-4* plants at low VPD, and significantly higher at high VPD (Figure 4). Photosynthetic apparatus was not compromised by the *crd-4* mutation with both WT-4 and *crd-4* plants having similar A-internal CO_2 concentration (C_i) relationships (Supplementary Figure S5). The lower maximum A observed in *crd-4* mutant plants is likely to have contributed to a reduction in shoot biomass observed in these plants compared to WT-4 plants (Supplementary Figure S6). Other factors may contribute to reduced growth in the *crd* mutants which, in addition to altered vein anatomy, have an occasional reduction or modification in tendril number as well as, rarely, leaflet/pinna number (Supplementary Figure S7 and S8).

Mutation in Crd *reduces auxin activity and levels in expanding leaves*

FMO enzymes are believed to catalyse the conversion of indole-3-pyruvic acid (IPyA) to auxin (indole-3-acetic acid (IAA)) (Mashiguchi et al., 2011). To visualise potential differences in auxin

Downloaded from on August 3, 2017 - Published by www.plantphysiol.org
Copyright © 2017 American Society of Plant Biologists. All rights reserved.

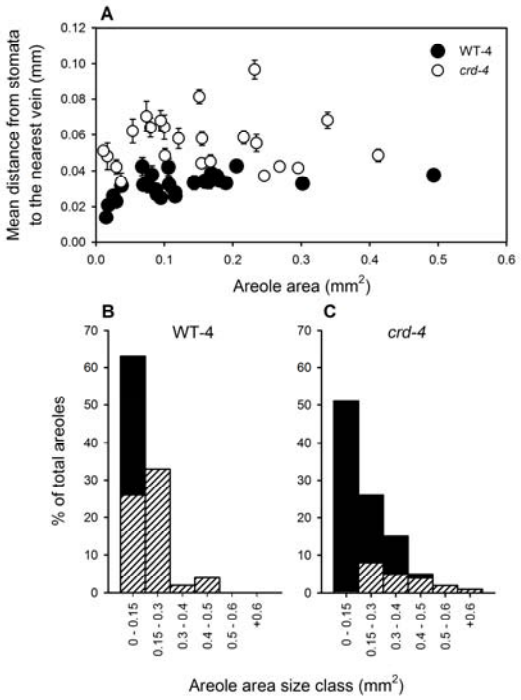

Figure 3. (A) The relationship between the mean distance from stomata to the nearest vein (including free ending veinlet) in an areole (±SE) and areole area for WT-4 (open circles) and *crd-4* mutant (closed circles) plants. Free ending veinlet occurrence across size classes of areoles in (B) WT-4 and (C) *crd-4* mutant plants; bars represent the percentage of areoles that fall within each size class, with hatching depicting the areoles in that size class that had free ending veinlets.

activity in the developing leaves of *crd-4* and WT-4 plants we utilised a *DR5::GUS* reporter construct, for which *GUS* expression is driven by the promoter of a highly active synthetic auxin response element (DeMason and Polowick, 2009). A substantial reduction in auxin activity was noted in the veins of developing leaves of *crd-4 DR::GUS* plants compared with those of WT-4 *DR5::GUS* plants, by minimal *GUS* staining (Figure 5A). In contrast to WT-4 leaves, no *GUS* staining was observed young leaves (less than 4 mm in length) of *crd-4 DR5::GUS* plants, indicating no auxin activity (Supplementary Figure S9). We further investigated this difference in auxin activity in developing leaves by quantifying the levels of both free IAA and the auxin conjugate, IAA-aspartate (IAAsp) in apical tissue containing developing leaves and meristematic tissue. Free IAA and IAAsp levels were reduced by approximately 50 and 80%, respectively, in the apical tissue of *crd-4* plants compared to WT-4 plants (Figure 5B and C). In contrast, a reduction in free IAA levels was not observed in whole shoots (Supplementary Figure S10).

Downloaded from on August 3, 2017 - Published by www.plantphysiol.org
Copyright © 2017 American Society of Plant Biologists. All rights reserved.

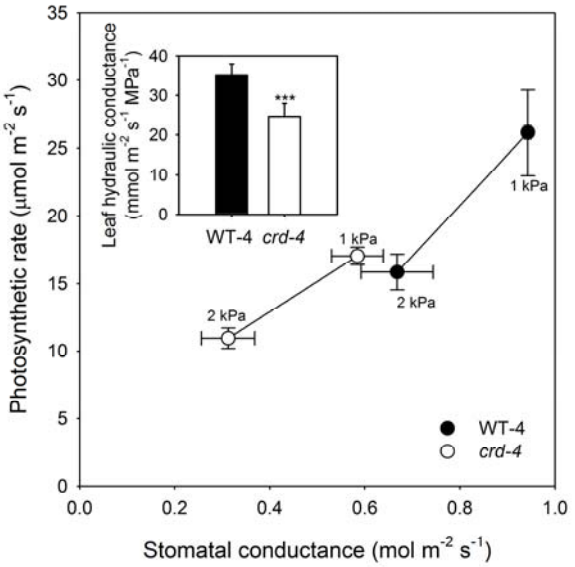

Figure 4. Mean photosynthetic rate and stomatal conductance (n=3; ±SE) measured in leaves of whole plants exposed to a vapour pressure deficit of 1 kPa or 2 kPa in WT-4 (black circles) and *crd-4* mutants (open circles). Insert depicts mean maximum leaf hydraulic conductance (n=6; ±SE) in WT-4 and *crd-4* mutant plants. Asterisks denote a significant difference in means (P<0.001).

Discussion

Auxin via vein anatomy drives maximum leaf gas exchange

Current theory indicates that the terminal path-length for water flow through the mesophyll should govern maximum K_{leaf} (Buckley et al., 2015), g_s and thus maximum A (Brodribb et al., 2010). However, both parts of this proposition are supported largely by correlative evidence, derived from natural variation within and between species (Sack and Frole, 2006; Brodribb et al., 2007; Brodribb and Feild, 2010; Scoffoni et al., 2015; Scoffoni et al., 2016). Recently, the influence of the distance through the mesophyll for water flow on K_{leaf} was demonstrated experimentally using a genetic approach (Caringella et al., 2015) and here we present genetic evidence that auxin, through leaf venation, acts as a regulator of both maximum leaf hydraulic supply and maximum A, and likely whole plant productivity. Our physiological analyses of the auxin-biosynthetic *crd* mutants indicate that altered vein density and topology results in an increase in the hydraulic path-length for water flow through the mesophyll, reduced maximum K_{leaf} and as a consequence maximum A. Our data support the conclusions derived from correlations that have highlighted the importance of an efficient internal leaf water transport system for maximising both g_s and A (Sack and Frole, 2006; Brodribb et al., 2007; Carins Murphy et al., 2012).

The effects of auxin deficiency on water transport, and consequently A, observed in the *crd-4* mutant, occurred independently of any changes in stomatal anatomy, photosynthetic apparatus or

Downloaded from on August 3, 2017 - Published by www.plantphysiol.org
Copyright © 2017 American Society of Plant Biologists. All rights reserved.

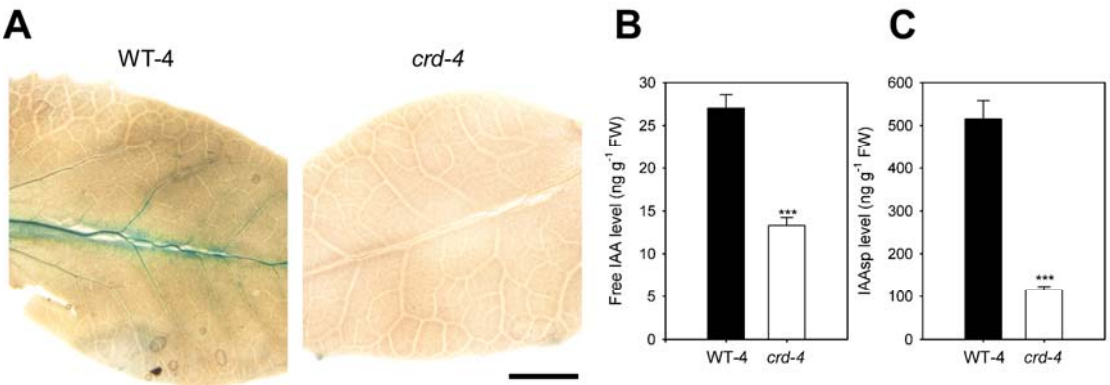

Figure 5. (A) GUS expression in expanding pinnae of representative F_2 segregant plants (less than 8 mm in length) taken from WT-4, *DR5::GUS* and *crd-4*, *DR5::GUS* plants (scale bar = 2 mm). (B) Mean levels of IAA and (C) IAAsp from apical tissue of WT-4 and *crd-4* mutant plants (n=4, ±SE). Asterisks denote a significant difference in means (P<0.001).

intrinsic photosynthetic capacity. This breaking of coordination between vein and stomatal development is surprising, given that angiosperms are extremely efficient at coordinating hydraulic supply (the formation of veins) with demand (the density of stomata) (Brodribb and Jordan, 2011; Carins Murphy et al., 2016). The absence of a distinctive stomatal phenotype in the *crd-4* mutant plants is at odds with the suggestion that auxin transport influences stomatal development (Le et al., 2014). Interestingly, there have been no reports of aberrant vein development in the collection of stomatal patterning mutants (Berger and Altmann, 2000; Kanaoka et al., 2008), which suggests independent pools of auxin are involved in the developmental regulation of these two morphological features. The endogenous signal that may be responsible for coordinating vein and stomatal density in a developing leaf thus remains unknown.

The formation of FEVs

In addition to providing experimental evidence for the link between maximum K_{leaf} and *A*, our observations of the *crd-4* mutant revealed substantial rearrangements in the topology of the leaf vein network. We found that, unlike in WT-4 plants, both major and minor vein density were reduced in mutant plants and in contrast to a wide diversity of angiosperms species (Fiorin et al., 2016), the development of FEVs in both large and small areoles in *crd-4* plants was affected, as evidenced by a greater distance from stomata to the nearest vein in all size classes of areoles. Recent work has suggested that a strong selective pressure is placed on plants to develop leaves with a uniform distance from the nearest vein to the stomata (Fiorin et al., 2016). The correct positioning of FEVs minimises the mean distance from the minor veins to the nearest stomata. The mechanism regulating this key anatomical feature of reticulate veined angiosperm leaves is unknown; however auxin clearly plays a major role.

Downloaded from on August 3, 2017 - Published by www.plantphysiol.org
Copyright © 2017 American Society of Plant Biologists. All rights reserved.

Auxin biosynthesis as a central regulator in the formation of veins

Auxin biosynthesis in plants occurs through a two-step pathway from the amino acid tryptophan to IAA via the intermediate IPyA (Zhao, 2012). These two steps are sequentially catalysed by tryptophan aminotransferases and FMOs from the YUCCA family (Tao et al., 2008; Mashiguchi et al., 2011). We show here that *Crd* is the only transcript recovered from *P. sativum* database searches that is embedded within the clade of FMO auxin biosynthetic genes including *YUCCA1* and *YUCCA4* from *A. thaliana* and *FLOOZY* from *Petunia* (Figure 1D). Consistent with this, we found reduced free IAA levels in *crd-4* apical tissue when compared with WT-4 plants (Figure 5B). This finding demonstrates the importance of local auxin synthesis in the early stages of leaf and vascular development. In addition to reduced IAA levels, our observation of substantially lower levels of IAAsp in the apical tissue of *crd-4*, compared to WT-4 plants, is indictative of impaired IAA biosynthesis in the apical bud. Interestingly, we observed no difference in free IAA levels in whole shoot tissue of seedlings of the *crd-4* mutant plants compared to WT-4 plants (Supplementary Figure S10), suggesting the reduction in auxin levels in these mutants is localised to the developing leaves. Our *DR5::GUS* reporter observations further support this, indicating that a reduction in IAA levels may be localised to the developing vascular tissue in expanding leaves of mutant plants (Figure 5A). In wild-type plants, high auxin activity in vascular tissue of developing leaves has been reported previously in pea (DeMason et al., 2013) as well as *Arabidopsis* (Mattsson et al., 2003); in *crd-4* leaves we found no *GUS* staining apparent in the developing veins (Figure 5A). Similar reductions in *GUS* staining have been observed in the veins of multiple *yuc* mutants in *Arabidopsis* lines carrying a *DR5::GUS* reporter (Cheng et al., 2006). Furthermore, systemic reductions in auxin activity were also noted in very young developing leaves of *crd-4* mutant plants (Supplementary Figure S9).

The development of the leaf vascular network can be explained by the auxin canalization theory, which describes a self-forming auxin transport stream initiating the formation of a vascular cambium (Sachs 1981). The profound and highly dysfunctional vein phenotypes of mutants in PIN-FORMED (PIN) proteins strongly implicate auxin efflux as a major regulator of this auxin transport stream and thus the formation of leaf veins (Mattsson et al., 1999). As a result, modifications to the auxin transport stream by auxin efflux dominates models seeking to simulate vein patterning (Bennet et al., 2014; Feugier et al., 2005; Lee et al., 2014; Mitchison, 1980; Rolland-Lagan and Prusinkiewicz, 2005). Our results, however, add to previous evidence suggesting that, in addition to auxin efflux rates, the biosynthesis of this hormone also plays an important role in establishing a normal leaf vascular network (Tobeña-Santamaria et al., 2002; Cheng et al., 2006; Cheng et al., 2007). Indeed, Cheng et al. (2007) found that auxin deficiency on a background of reduced auxin efflux had an additive effect

Downloaded from on August 3, 2017 - Published by www.plantphysiol.org
Copyright © 2017 American Society of Plant Biologists. All rights reserved.

on compromised leaf vascular development. Whether current models for leaf venation patterning, based primarily on auxin efflux dynamics, can mimic venation patterns observed in auxin biosynthetic mutants or require substantial modification will be an interesting avenue for future research.

Auxin as a driver of maximum photosynthetic rate

The importance of *Crd*, a FMO, in normal vein formation and thus maximum *A* suggests that this clade of auxin biosynthetic genes have been central to the formation of complex, high density vein networks in the leaves of derived angiosperms, a prerequisite for the high productivity of these species (Scoffoni et al., 2016). Phylogenetic analysis of closely related FMOs suggests that duplication and functional specialisation in this family occurred prior to and during the diversification of angiosperms, allowing for the evolution of a clade of genes that play key roles in the development and topology of veins. This clade includes *Crispoid*, Ph*FLOOZY*, At*YUCCA1* and At*YUCCA4*, which all result in compromised leaf vascular development when mutated (Tobeña-Santamaria et al., 2002; Cheng et al., 2006; Cheng et al., 2007). Given the importance of auxin in the development of efficient reticulate venation patterns in angiosperms, it is an intriguing possibility that this hormone may have played an instrumental role in the Cretaceous radiation and ecological rise of the angiosperms. Indeed as the hydraulic pathway through the leaf accounts for the greatest limitation to maximum realised leaf gas exchange, whether enhancing auxin levels in a developing leaf will improve maximum productivity remains to be tested. However, our new mechanistc understanding of auxin as a key developmental determinant of maximum leaf gas exchange provides exciting potential for future increases in plant productivity.

Materials and Methods

Plant material

Previously described *crd* mutants include the first described allele (*crd-1*; JI 2460) selected afterN-ethyl-N-nitrosourea mutagenesis of the line Paloma (WT-1) (Swiecicki, 1989) and the *crispoid-whip* allele (*crd-2*; JI 3160), found after ethyl methane sulfonate (EMS) mutagenesis of the line SG (WT-2) (Berdnikov et al., 2000). These mutants were obtained from the John Innes Pisum Germplasm collection. In this paper, two novel *crd* mutant alleles were identified. The *crd-3* mutant was identified as line FN 1522/1 in a fast neutron mutagenesis population of the JI 2822 line (WT-3) (Domoney et al., 2013). The *crd-4* mutant was observed incidentally in line 905, derived from an EMS mutagenesis population of the Caméor line in the UTILLdb programme (Dalmais et al., 2008). Initially this mutant was named *pipes in short supply* (*pss*). Allelism was confirmed by non-

Downloaded from on August 3, 2017 - Published by www.plantphysiol.org
Copyright © 2017 American Society of Plant Biologists. All rights reserved.

complementation of the *crd* phenotype in F_1 progeny from the crosses of FN1522/1 x *crd1*, FN1522/1 x *crd2* and *pss* x *crd1* (Supplementary Figure S1). At least six generations of backcross selection were undertaken to provide near-isogenic wild-type (WT-4) and *crd-4* lines for morphological and physiological experiments. Three generations of backcross selection were undertaken to provide *crd-3* lines for RNA sequencing.

crd-1, *crd-2*, *crd-3* and respective wild-type plants (as well as plants from allelism tests between these lines) were sown in a glasshouse in Aberystwyth, United Kingdom, under natural light between June and September (5.2-9.5/18.2-22.4°C day/night temperatures), in peat-free Jiffy pellets 7C, 45x40mm (Jiffy products S.L. (pvt) Ltd) and after two weeks transferred into 12 cm long and 12 cm diameter pots with John Innes potting mix number 3 (http://www.johninnes.info/about.htm) supplemented with 30% chick grit. Jiffy pellets and pots were placed on a carpet which was watered everyday, allowing the plants to absorb water through the carpet. WT-4 and *crd-4* plants (and plants for the allelism test with this line, as well as *DR5::GUS* reporter lines) were grown under the controlled glasshouse conditions in Hobart, Australia, described by McAdam et al. (2016). All morphological and physiological observations were made on fully expanded node 4 leaves, unless specified otherwise.

RNA-sequencing and sequence data analysis to identify the crd-3 *mutation*

Total RNA from 20 day-old *crd-3* and WT-3 shoot tips (three replicates each) was extracted using the RNeasy Plant Mini Kit (Qiagen) and RNA concentration was determined using a Qubit fluorescence spectrophotometer (Thermo Fischer). Each amplified library for sequencing was prepared from 2ug of total RNA (Illumina TruSeq RNA v2 Sample Preparation Kit) and uniquely indexed to enable multiplex sequencing. Libraries were analysed by gel electrophoresis and quantified using Qubit then adjusted to 10nM in 0.1M Tris-HCl/0.01% (v/v) Tween 20 buffer and pooled equally prior to denaturation/dilution in a final loading concentration of 8pM. Uniquely indexed, amplified libraries prepared for RNA-seq were typically 300 bp in size. These were multiplexed and sequenced in 2x126bp format in a single lane of a HiSeq v4 high-output flowcell on an Illumina HiSeq2500 platform. Data in FASTQ format was analysed using the Genomics Workbench v6.5 software package (CLC Bio). RNA-seq data obtained ranged from 68.3 to 79.5 million reads per sample for *crd-3* (average 73 million) and from 73 to 90 million reads for WT-3 (average 80.4 million). Following trimming to remove low-quality sequence and reads <50bp, these were reduced to an average of 71.4 million reads for *crd-3* and 78.9 million reads for WT-3, with an average read length of 113bp for all samples. Overlapping WT-3 read-pairs were merged (~54% of each WT dataset), and this data

Downloaded from on August 3, 2017 - Published by www.plantphysiol.org
Copyright © 2017 American Society of Plant Biologists. All rights reserved.

was used along with unmerged WT-3 read-pairs (21.85 Gbp in total) for *de novo* assembly of a reference transcriptome using the *de Bruijn* graph method with a k-mer value of 25. Maximum bubble size for conflict resolution within the graph was set at 50. Repeat regions within the graph were resolved using scaffolding based on paired-end sequences. Following initial contig assembly, reads were mapped back to contigs, requiring 50% identity and 80% similarity across the read. Ambiguous reads mapping to more than one contig were discarded. Insertion and deletion penalties were set at 3 and mismatch penalty at 2. Contigs from the initial assembly were removed if no reads mapped. Reads from all six individual samples were subsequently mapped to these reference contigs and used to calculate the number of reads mapped per kb of exon, per million mapped reads (RPKM) (Mortazavi et al., 2008). On average, 85% of reads from each sample could be mapped to reference contigs and used to generate RPKM expression values. RPKM values were analysed as a two-group experiment, *crd-3* vs WT-3, to identify significantly different expression values between the two groups, with p-values adjusted using a false-discovery rate (FDR) (Benjamini and Hochberg, 1995). One significantly different (FDR corrected p-value < 0.05) contig sequence, showing complete absence of expression in *crd-3* mutants, was used to query NCBI nucleotide and protein databases, using BLASTn and BLASTx, respectively, in order to identify the corresponding gene.

Sanger sequencing for mutant characterisation

For cDNA template preparation, total RNA was first extracted as for RNA-sequencing and treated with DNase (Ambion; WT-1 to -3, *crd-1* to *-3*), or with the SV total RNA isolation system (Promega) including a DNase step (WT-4, *crd-4*), and quality-checked by gel electrophoresis. RNA was reverse-transcribed using oligo-dT primers and the Superscript III First-Strand Synthesis System (Invitrogen) in a total volume of 50 µl containing 0.4 µg RNA (WT-1 and *crd-1*) or 0.2µg RNA (WT-2 and *crd-2*; WT-3 and *crd-3*), or using the Tetro cDNA synthesis kit (Bioline) in 20 µL containing 1 µg RNA (WT-4 and *crd-4*). Genomic DNA template was extracted from leaves following the DNeasy Plant Mini Kit protocol (Qiagen; WT-1 to -3, *crd-1* to *-3*) or using a CTAB-based method (WT-4, *crd-4*) (Allen et al., 2006). All primers are listed in Supplementary Table S3. Sanger sequencing of purified PCR products was performed at Aberystwyth University or by Macrogen Inc. (Korea).

Genetic Analysis

Plants grown in the glasshouse were scored for *crd* or WT phenotype. A WT-1 x *crd-1* cross yielded 96 F_3 progeny segregating 74:22 (3:1, χ^2= 0.2, P > 0.6, n.s.). To test for co-segregation of the *crd* phenotype and the *crd-1* mutation, phenotype and genotype scores of the F_3 progeny were compared. Genomic DNA prepared from each plant was genotyped using a cleaved-amplified

Downloaded from on August 3, 2017 - Published by www.plantphysiol.org
Copyright © 2017 American Society of Plant Biologists. All rights reserved.

polymorphic sequence (CAPS) marker for the *Crd* locus, amplified by PCR using primers 5F and 7R in Supplemental Table 1 and digested with *Dde*I. Digestion products were distinguished after gel electrophoresis (WT-1: 385 bp, 147 bp and 110 bp; *crd-1*: 385 bp and 257 bp). All plants homozygous for the *crd-1* allele had the *crd* phenotype and no heterozygous plant nor any plants homozygous for the WT-1 allele had the *crd* phenotype (χ^2= 93.2, P = 6 x 10^{-21}). The same CAPS marker was used to place the *Crd* locus on the genetic map of the JI 281 x JI 399 recombinant imbred population (Laucou et al., 1998) at position 130 cM on LG II, between markers *cDNA39* and *SNP190*.

Phylogenetic analysis

The phylogenetic relationships between *YUCCA*-related genes in *Arabidopsis thaliana*, *Medicago truncatula* and *P. sativum* were assessed in conjunction with selected characterised genes from other species using amino acid sequences obtained from GenBank (www.ncbi.nlm.nih.gov) and the *P. sativum* gene atlas (Alves-Carvalho et al., 2015) (Supplementary Table S2). Sequences were aligned using the Clustal Omega algorithm (Sievers et al., 2011) and phylogenies were reconstructed using an LG substitution model (Le and Gascuel, 2008) based on a BIONJ tree using the statistical analysis software 'R'. The packages APE (Paradis et al., 2004) and phangorn (Schliep, 2011) were used for sequence management and modelling, and ggtree (Yu et al., 2017) was used for tree visualisation.

Leaf anatomy

Leaves of *crd-1*, *crd-2* and *crd-3* mutant lines and respective wild-types were prepared for vein density measurements by incubating overnight in a solution of 3:1 ethanol:acetic acid (v v^{-1}) at room temperature. Leaves were then incubated for 1 h in a solution of 70% ethanol in water (v v^{-1}) and later transferred to 50% ethanol in water (v v^{-1}) until scanned at 600-1200 DPI (HP Scanjet 8200).

Paradermal section of WT-4 and *crd-4* leaves were cleared in household bleach (50 g L^{-1} sodium hypochlorite and 13 g L^{-1} sodium hydroxide) and stained in 1% toluidine blue. Five fields of view (FOV) at 4x magnification (for vein density measurements, FOV: 3.47 mm^2), five FOV at 20x magnification (for stomatal density measurements), sufficient images at 40x magnification to capture 50 stomata (for measuring stomatal size) and images at 20x magnification focusing on the abaxial stomatal surface and covering the entire areole (for calculating mean stomatal distance to the nearest vein) were taken using a Nikon Digital Sight DS-L1 camera (Melville, NY, USA) mounted on a Leica DM 1000 microscope (Nussloch, Germany). Vein density and stomatal density were measured using ImageJ, as the total length of leaf vascular tissue and total number of stomata per mm^2 of leaf area. Stomatal size was determined by measuring the longest distance parallel to the stomatal pore from the edges of the guard cells using ImageJ. The mean distance from stomata to

Downloaded from on August 3, 2017 - Published by www.plantphysiol.org
Copyright © 2017 American Society of Plant Biologists. All rights reserved.

the nearest vein for 24 areoles, randomly selected to span the full size spectrum of areoles across the leaf, was determined by making a composite image of each areole using the 20x objective FOVs which were then assembled together in Adobe Photoshop. This composite image of each areole was analysed using specifically designed software that calculated the mean distance to the nearest vein for each stomata in the areole once veins and stomata were manually marked. Leaf cross-sections were made from leaf segments spanning the midrib that were fixed in 2.5% buffered glutaraldehyde under vacuum then dehydrated in acetone and embedded in Spurr's resin. Semi-thick sections (5-7 µm) were stained with toluidine blue O.

Leaf gas exchange and hydraulic conductance

One leaf from three individuals of both WT-4 and *crd-4* were used to determine the response of leaf gas exchange to variation in vapour pressure deficit (VPD). A portable infrared gas analyser (Li-6400; Li-Cor Biosciences) was used to measure leaf gas exchange between 1130 and 1300 h when gas exchange was expected to be maximal. Conditions within the leaf cuvette were maintained as close to external conditions as possible (temperature at 22°C and light intensity at 1000 µmol m^{-2} s^{-1}, VPD was regulated relative to external conditions by controlling intake air flow through a desiccant column). On the first day of measurement, VPD in the glasshouse was held at 1 kPa from dawn by a dehumidifier with integrated humidity sensors (ADH-1000, Airrex Portable dehumidifier, Hephzibah Co. Ltd.), on the second day of measurement VPD in the glasshouse was held at 2 kPa. On each day, midday leaf water potential was measured in all plants using a pressure chamber. K_{leaf} was measured in three leaves of WT-4 and *crd-4* plants using the evaporative flux method and flow meter according to Carins Murphy et al. (2012).

Shoot biomass and growth

Whole shoots of WT-4 and *crd-4* plants (n=3), grown under the same glasshouse conditions, were harvested 28 days after sowing and dried at 70°C for at least 62 h before being weighed (±0.0001 g). Plant height in WT-1, *crd-1*, WT-3 and *crd-3* plants (n=13-14), grown under the same glasshouse conditions, was measured every 10 days (from 20 days after sowing) until plants had dried at 60 days after sowing.

Quantification of free IAA and IAAsp levels

Growing apical tissue, including all tissues immediately proximal to the uppermost fully expanded leaf of WT-4 and *crd-4* plants, were harvested. Tissue was weighed (± 0.0001g; with approximately 25 mg harvested per replicate for both genotypes) and placed in 1 mL of sodium phosphate buffer (50nM, pH7). Samples were homogenised with a bead mill for 2 minutes. To quantify the

Downloaded from on August 3, 2017 - Published by www.plantphysiol.org
Copyright © 2017 American Society of Plant Biologists. All rights reserved.

endogenous compounds, stable isotope-labeled internal standards were added, these were [$^{13}C_6$]-IAA (Cambridge Isotope Laboratories, Tewksbury, MA, USA) and [^{15}N, $^{2}H_5$]-IAAsp (OlChemim, Olomouc, Czech Republic). Compounds were extracted according to Novák *et al*. (2012). In addition, free auxin was quantified in two week old whole seedlings of WT-4 and *crd-4*, which were weighed and harvested into 3 mL of 80% methanol in water (v v^{-1}) containing 250 mg L^{-1} butylated hydroxytoluene. All samples were analysed by ultra-performance liquid chromatography tandem mass spectrometry (UPLC-MS/MS) as described by Cook *et al*. (2016).

DR5::GUS *staining for auxin activity*

Transgenic *DR5::GUS* lines carrying the *Crd-4* and *crd-4* alleles were constructed by crossing the RTP9 line (DeMason and Polowick, 2009) with *crd-4* mutant pollen. The segregating F_2 generation consisting of 42 *Crd* GUS+: 15 *crd* GUS+: 14 *Crd* GUS-: 7 *crd* GUS- (9:3:3:1, χ^2 = 1.0, P=0.8, n.s.) was genotyped by PCR for *DR5::GUS* using the primers and conditions described by DeMason and Polowick (2009) and distinctive leaf morphology phenotypes were used to identify *crd-4* plants. Young developing leaflets less than 8 mm in length, (one per individual, harvested from 8 randomly selected individuals per genotype) were removed from within stipules enclosing the apical meristem and immediately immersed in GUS staining buffer containing 2 mM 5-bromo- 4-chloro-3-indolyl b-D-glucuronide, 100 mM sodium phosphate (pH 7.5), 0.5 mM potassium ferricyanide, 0.5 mM potassium ferrocyanide, 10 mM EDTA, and 0.1% (v/v) Triton X-100. Samples were vacuum-infiltrated on ice at 200 mbar for 45 minutes then incubated for 48 hours at 37°C. The staining buffer was refreshed after 24 hours. The samples were then cleared in 70% ethanol, dissected and photographed as described above. To ensure an unbiased methodological approach and morphological assessment of *GUS* staining in the leaves, the samples were stained, cleared and photographed without prior knowledge of the genotype using a double-blind methodology. After decoding the genotypes, staining was compared in 3 randomly selected leaflets of less than 4 mm in length from *crd-4* and WT plants carrying the *DR5::GUS* reporter, in addition to a randomly selected leaflet less than 8 mm in length from each of the two genotypes.

Downloaded from on August 3, 2017 - Published by www.plantphysiol.org
Copyright © 2017 American Society of Plant Biologists. All rights reserved.

Supplementary materials

Supplementary Figure S1: Representative images of leaves or leaflets from F1 plants of crosses between putative mutant lines carrying the *crd* phenotype.

Supplementary Figure S2. The G628A SNP in *crd-2* affects *PsYUC1* splicing.

Supplementary Figure S3. Alignment of Crispoid protein from three wild-type and mutant lines.

Supplementary Figure S4: No portion of *Crispoid*/*PsYUC1* could be amplified from *crd-3* mutant genomic DNA template.

Supplementary Figure S5. Photosynthetic rate/internal CO_2 concentration curves for WT-4 and *crd-4* mutant plants.

Supplementary Figure S6. Mean dry shoot biomass and plant height in WT and *crd* plants.

Supplementary Figure S7. Missing and under-developed tendrils in the *crd-1* mutant leaves.

Supplementary Figure S8. Missing and under-developed tendrils and pinnae in leaves of the *crd-3* mutant.

Supplementary Figure S9. GUS expression in F2 segregant plants.

Supplementary Figure S10. Mean levels of free indole-3-acetic acid from whole aerial potions of 14 day old seedlings of WT-4 and *crd-4* mutant plants.

Supplementary Table S1. Mean secondary and tertiary vein densities in leaves of allelic *crd* mutants and respective wild-types.

Supplementary Table S2. Accession numbers of proteins used for phylogenetic analysis.

Supplementary Table S3. Details of *Crd* primers used in this study.

Acknowledgements

The authors would like to thank Charly Potter for preparation of libraries for RNA-seq, Caron James for Sanger sequencing, Vincent Vadez for helpful discussions, Patricia Polowick for generously providing the RTP9 line carrying the *DR5::GUS* insert, Noel Ellis for statistical advice and comments on the manuscript and two reviewers for astute recommendations on auxin quantifications.

Downloaded from on August 3, 2017 - Published by www.plantphysiol.org
Copyright © 2017 American Society of Plant Biologists. All rights reserved.

Figure Legends

Figure 1. (A) Representative leaflets from node 6 taken from each *crd* mutant allele and respective wild-type. A 1 cm scale marker for each pair is shown in the wild-type image of each pairing. (B) Aerial view of seedlings of WT-3 and *crd-3* (left) and WT-4 and *crd-4* (right) showing node 4 leaves uppermost in each panel. A 2 cm scale marker for each pair of images is shown on the mutant image of each pairing. Similar images or comprehensive phenotypic details of *crd-1* and *crd-2* seedlings are provided by Swiecicki (1989) and Berdnikov et al. (2000), respectively. (C) Diagram of *Crd* gene showing regions encoding conserved motifs and the positions of *crd* mutations. Exons are shown as boxes, nucleotides encoding FAD- and NADPH-binding motifs are shown as black bars, ATG-containing motif 1 is shown as a grey bar. (D) Phylogenetic analysis of YUCCA protein sequences from *M. truncatula* (Mt), *P. sativum* (Ps) and *A. thaliana* (At), as well as ToFZY (*Solanum lycopersicum*), PhFLOOZY (*Petunia x hybrida*). Bootstrap values (from 1000 iterations) for this BIONJ tree are displayed adjacent to nodes and the scale bar indicates genetic distance (0.25 changes/amino acid). Diamonds indicate collapsed clades belonging to the putative, but uncharacterised seed YUCCA clades. Accession numbers for all genes are given in Supplementary Table S2.

Figure 2. (A) A representative longitudinal image of leaf venation in WT-4 and *crd-4* leaves (scale bar = 200 µm, red lines outline an areole, blue lines highlight free ending veinlets within the areole). (B) A representative cross-sectional image of WT-4 and *crd-4* mutant leaves through the midrib (scale bar = 200 µm). (C) Mean vein density (n=7 leaves, ±SE), (D) stomatal density (n=7 leaves, ±SE) and (E) stomatal size (n=50 stomata, ±SE) in WT-4 and *crd-4* mutant plants. Asterisks denote significant difference in means ($P<0.001$).

Figure 3. (A) The relationship between the mean distance from stomata to the nearest vein (including free ending veinlet) in an areole (±SE) and areole area for WT-4 (open circles) and *crd-4* mutant (closed circles) plants. Free ending veinlet occurrence across size classes of areoles in (B) WT-4 and (C) *crd-4* mutant plants; bars represent the percentage of areoles that fall within each size class, with hatching depicting the areoles in that size class that had free ending veinlets.

Figure 4. Mean photosynthetic rate and stomatal conductance (n=3; ±SE) measured in leaves of whole plants exposed to a vapour pressure deficit of 1 kPa or 2 kPa in WT-4 (black circles) and *crd-4* mutants (open circles). Insert depicts mean maximum leaf hydraulic conductance (n=6; ±SE) in WT-4 and *crd-4* mutant plants. Asterisks denote a significant difference in means ($P<0.001$).

Downloaded from on August 3, 2017 - Published by www.plantphysiol.org
Copyright © 2017 American Society of Plant Biologists. All rights reserved.

Figure 5. (A) GUS expression in expanding pinnae of representative F_2 segregant plants (less than 8 mm in length) taken from WT-4, *DR5::GUS* and *crd-4, DR5::GUS* plants (scale bar = 2 mm). (B) Mean levels of IAA and (C) IAAsp from apical tissue of WT-4 and *crd-4* mutant plants (n=4, ±SE). Asterisks denote a significant difference in means ($P<0.001$).

Downloaded from on August 3, 2017 - Published by www.plantphysiol.org
Copyright © 2017 American Society of Plant Biologists. All rights reserved.

Parsed Citations

Allen GC, Flores-Vergara MA, Krasynanski S, Kumar S, Thompson WF (2006) A modified protocol for rapid DNA isolation from plant tissues using cetyltrimethylammonium bromide. Nat Protocols 1: 2320-2325

Pubmed: Author and Title
CrossRef: Author and Title
Google Scholar: Author Only Title Only Author and Title

Alves-Carvalho S, Aubert G, Carrère S, Cruaud C, Brochot A-L, Jacquin F, Klein A, Martin C, Boucherot K, Kreplak J, da Silva C, Moreau S, Gamas P, Wincker P, Gouzy J, Burstin J (2015) Full-length de novo assembly of RNA-seq data in pea (Pisum sativum L.) provides a gene expression atlas and gives insights into root nodulation in this species. Plant J 84: 1-19

Pubmed: Author and Title
CrossRef: Author and Title
Google Scholar: Author Only Title Only Author and Title

Benjamini Y, Hochberg Y (1995) Controlling the false discovery rate: a practical and powerful approach to multiple testing. Journal of the Royal Statistical Society. Series B (Methodological) 57: 289-300

Pubmed: Author and Title
CrossRef: Author and Title
Google Scholar: Author Only Title Only Author and Title

Bennett T, Hines G, Leyser O (2014) Canalization: what the flux? Trends in Genetics 30: 41-48

Pubmed: Author and Title
CrossRef: Author and Title
Google Scholar: Author Only Title Only Author and Title

Berdnikov VA, Gorel' FL, Kosterin OE (2000) A new allele at Crd distrubs development of the compound leaf. Pisum Genetics 32: 6-8

Pubmed: Author and Title
CrossRef: Author and Title
Google Scholar: Author Only Title Only Author and Title

Berger D, Altmann T (2000) A subtilisin-like serine protease involved in the regulation of stomatal density and distribution in Arabidopsis thaliana. Genes Dev 14: 1119-1131

Pubmed: Author and Title
CrossRef: Author and Title
Google Scholar: Author Only Title Only Author and Title

Boyce CK, Brodribb TJ, Feild TS, Zwieniecki MA (2009) Angiosperm leaf vein evolution was physiologically and environmentally transformative. Proc R Soc Lond B Biol Sci 276: 1771-1776

Pubmed: Author and Title
CrossRef: Author and Title
Google Scholar: Author Only Title Only Author and Title

Brodribb TJ, Feild TS (2000) Stem hydraulic supply is linked to leaf photosynthetic capacity: evidence from New Caledonian and Tasmanian rainforests. Plant Cell Environ 23: 1381-1388

Pubmed: Author and Title
CrossRef: Author and Title
Google Scholar: Author Only Title Only Author and Title

Brodribb TJ, Feild TS (2010) Leaf hydraulic evolution led a surge in leaf photosynthetic capacity during early angiosperm diversification. Ecol Lett 13: 175-183

Pubmed: Author and Title
CrossRef: Author and Title
Google Scholar: Author Only Title Only Author and Title

Brodribb TJ, Feild TS, Jordan GJ (2007) Leaf maximum photosynthetic rate and venation are linked by hydraulics. Plant Physiol 144: 1890-1898

Pubmed: Author and Title
CrossRef: Author and Title
Google Scholar: Author Only Title Only Author and Title

Brodribb TJ, Feild TS, Sack L (2010) Viewing leaf structure and evolution from a hydraulic perspective. Funct Plant Biol 37: 488-498

Pubmed: Author and Title
CrossRef: Author and Title
Google Scholar: Author Only Title Only Author and Title

Brodribb TJ, Holbrook NM (2005) Water stress deforms tracheids peripheral to the leaf vein of a tropical conifer. Plant Physiol 137: 1139-1146

Pubmed: Author and Title
CrossRef: Author and Title
Google Scholar: Author Only Title Only Author and Title

Brodribb TJ, Holbrook NM, Zwieniecki MA, Palma B (2005) Leaf hydraulic capacity in ferns, conifers and angiosperms: Impacts on photosynthetic maxima. New Phytol 165: 839-846

Pubmed: Author and Title
CrossRef: Author and Title
Google Scholar: Author Only Title Only Author and Title

Brodribb TJ, Jordan GJ (2011) Water supply and demand remain balanced during leaf acclimation of Nothofagus cunninghamii

Downloaded from www.plantphysiol.org
Copyright © 2017 American Society of Plant Biologists. All rights reserved.

trees. New Phytol 192: 437-448
Pubmed: Author and Title
CrossRef: Author and Title
Google Scholar: Author Only Title Only Author and Title

Buckley TN, John GP, Scoffoni C, Sack L (2015) How does leaf anatomy influence water transport outside the xylem? Plant Physiol 168: 1616-1635
Pubmed: Author and Title
CrossRef: Author and Title
Google Scholar: Author Only Title Only Author and Title

Caringella MA, Bongers FJ, Sack L (2015) Leaf hydraulic conductance varies with vein anatomy across Arabidopsis thaliana wild-type and leaf vein mutants. Plant Cell Environ 38: 2735-2746
Pubmed: Author and Title
CrossRef: Author and Title
Google Scholar: Author Only Title Only Author and Title

Carins Murphy MR, Jordan GJ, Brodribb TJ (2012) Differential leaf expansion can enable hydraulic acclimation to sun and shade. Plant Cell Environ 35: 1407-1418
Pubmed: Author and Title
CrossRef: Author and Title
Google Scholar: Author Only Title Only Author and Title

Carins Murphy MR, Jordan GJ, Brodribb TJ (2016) Cell expansion not cell differentiation predominantly co-ordinates veins and stomata within and among herbs and woody angiosperms grown under sun and shade. Ann Bot
Pubmed: Author and Title
CrossRef: Author and Title
Google Scholar: Author Only Title Only Author and Title

Cheng Y, Dai X, Zhao Y (2006) Auxin biosynthesis by the YUCCA flavin monooxygenases controls the formation of floral organs and vascular tissues in Arabidopsis. Genes Dev 20: 1790-1799
Pubmed: Author and Title
CrossRef: Author and Title
Google Scholar: Author Only Title Only Author and Title

Cheng Y, Dai X, Zhao Y (2007) Auxin synthesized by the YUCCA flavin monooxygenases is essential for embryogenesis and leaf formation in Arabidopsis. Plant Cell 19: 2430-2439
Pubmed: Author and Title
CrossRef: Author and Title
Google Scholar: Author Only Title Only Author and Title

Cook SD, Nichols DS, Smith J, Chourey PS, McAdam EL, Quittenden L, Ross JJ (2016) Auxin biosynthesis: are the indole-3-acetic acid and phenylacetic acid biosynthesis pathways mirror images? Plant Physiol 171: 1230-1241
Pubmed: Author and Title
CrossRef: Author and Title
Google Scholar: Author Only Title Only Author and Title

Dalmais M, Schmidt J, Le Signor C, Moussy F, Burstin J, Savois V, Aubert G, Brunaud V, de Oliveira Y, Guichard C, Thompson R, Bendahmane A (2008) UTILLdb, a Pisum sativum in silico forward and reverse genetics tool. Genome Biol 9: R43-R43
Pubmed: Author and Title
CrossRef: Author and Title
Google Scholar: Author Only Title Only Author and Title

DeMason DA, Chetty V, Barkawi LS, Liu X, Cohen JD (2013) Unifoliata-Afila interactions in pea leaf morphogenesis. Am J Bot 100: 478-495
Pubmed: Author and Title
CrossRef: Author and Title
Google Scholar: Author Only Title Only Author and Title

DeMason Darleen A, Polowick Patricia L (2009) Patterns of DR5::GUS expression in organs of pea (Pisum sativum). Int J Plant Sci 170: 1-11
Pubmed: Author and Title
CrossRef: Author and Title
Google Scholar: Author Only Title Only Author and Title

Domoney C, Knox M, Moreau C, Ambrose M, Palmer S, Smith P, Christodoulou V, Isaac PG, Hegarty M, Blackmore T, Swain M, Ellis N (2013) Exploiting a fast neutron mutant genetic resource in Pisum sativum (pea) for functional genomics. Funct Plant Biol 40: 1261-1270
Pubmed: Author and Title
CrossRef: Author and Title
Google Scholar: Author Only Title Only Author and Title

Feugier FG, Mochizuki A, Iwasa Y (2005) Self-organization of the vascular system in plant leaves: Inter-dependent dynamics of auxin flux and carrier proteins. J Theor Biol 236: 366-375
Pubmed: Author and Title
CrossRef: Author and Title
Google Scholar: Author Only Title Only Author and Title

Fiorin L, Brodribb TJ, Anfodillo T (2016) Transport efficiency through uniformity: organization of veins and stomata in angiosperm leaves. New Phytol 209: 216-227

Downloaded from on August 3, 2017 - Published by www.plantphysiol.org
Copyright © 2017 American Society of Plant Biologists. All rights reserved.

Pubmed: Author and Title
CrossRef: Author and Title
Google Scholar: Author Only Title Only Author and Title

Fujino K, Matsuda Y, Ozawa K, Nishimura T, Koshiba T, Fraaije MW, Sekiguchi H (2008) NARROW LEAF 7 controls leaf shape mediated by auxin in rice. Mol Genet Genomics 279: 499-507
Pubmed: Author and Title
CrossRef: Author and Title
Google Scholar: Author Only Title Only Author and Title

Kanaoka MM, Pillitteri LJ, Fujii H, Yoshida Y, Bogenschutz NL, Takabayashi J, Zhu J-K, Torii KU (2008) SCREAM/ICE1 and SCREAM2 specify three cell-state transitional steps leading to Arabidopsis stomatal differentiation. Plant Cell 20: 1775-1785
Pubmed: Author and Title
CrossRef: Author and Title
Google Scholar: Author Only Title Only Author and Title

Laucou V, Haurogné K, Ellis N, Rameau C (1998) Genetic mapping in pea. 1. RAPD-based genetic linkage map of Pisum sativum. Theor Appl Genet 97: 905-915
Pubmed: Author and Title
CrossRef: Author and Title
Google Scholar: Author Only Title Only Author and Title

Le J, Liu X-G, Yang K-Z, Chen X-L, Zou J-J, Wang H-Z, Wang M, Vanneste S, Morita M, Tasaka M, Ding Z-J, Friml J, Beeckman T, Sack F (2014) Auxin transport and activity regulate stomatal patterning and development. Nat Commun 5: 3090
Pubmed: Author and Title
CrossRef: Author and Title
Google Scholar: Author Only Title Only Author and Title

Le SQ, Gascuel O (2008) An Improved General Amino Acid Replacement Matrix. Mol Biol Evol 25: 1307-1320
Pubmed: Author and Title
CrossRef: Author and Title
Google Scholar: Author Only Title Only Author and Title

Lee S-W, Feugier FG, Morishita Y (2014) Canalization-based vein formation in a growing leaf. J Theor Biol 353: 104-120
Pubmed: Author and Title
CrossRef: Author and Title
Google Scholar: Author Only Title Only Author and Title

Liu H, Ying Y-Y, Zhang L, Gao Q-H, Li J, Zhang Z, Fang J-G, Duan K (2012) Isolation and characterization of two YUCCA flavin monooxygenase genes from cultivated strawberry (Fragaria × ananassa Duch.). Plant Cell Rep 31: 1425-1435
Pubmed: Author and Title
CrossRef: Author and Title
Google Scholar: Author Only Title Only Author and Title

Mashiguchi K, Tanaka K, Sakai T, Sugawara S, Kawaide H, Natsume M, Hanada A, Yaeno T, Shirasu K, Yao H, McSteen P, Zhao Y, Hayashi K-i, Kamiya Y, Kasahara H (2011) The main auxin biosynthesis pathway in Arabidopsis. Proc Natl Acad Sci USA 108: 18512-18517
Pubmed: Author and Title
CrossRef: Author and Title
Google Scholar: Author Only Title Only Author and Title

Mattsson J, Ckurshumova W, Berleth T (2003) Auxin signaling in Arabidopsis leaf vascular development. Plant Physiol 131: 1327-1339
Pubmed: Author and Title
CrossRef: Author and Title
Google Scholar: Author Only Title Only Author and Title

Mattsson J, Sung ZR, Berleth T (1999) Responses of plant vascular systems to auxin transport inhibition. Development 126: 2979-2991.
Pubmed: Author and Title
CrossRef: Author and Title
Google Scholar: Author Only Title Only Author and Title

McAdam SAM, Brodribb TJ, Ross JJ (2016) Shoot-derived abscisic acid promotes root growth. Plant Cell Environ 39: 652-659
Pubmed: Author and Title
CrossRef: Author and Title
Google Scholar: Author Only Title Only Author and Title

Mitchison GJ (1980) Model for vein formation in higher-plants. Proc R Soc Lond B Biol Sci 207: 79-109
Pubmed: Author and Title
CrossRef: Author and Title
Google Scholar: Author Only Title Only Author and Title

Mortazavi A, Williams BA, McCue K, Schaeffer L, Wold B (2008) Mapping and quantifying mammalian transcriptomes by RNA-Seq. Nat Methods 5: 621-628
Pubmed: Author and Title
CrossRef: Author and Title
Google Scholar: Author Only Title Only Author and Title

Novák O, Hényková E, Sairanen I, Kowalczyk M, Posíšil T, and Ljung K (2012). Tissue-specific profiling of the Arabidopsis thaliana auxin metabolome. Plant J 72: 523-536.
Downloaded from on August 3, 2017 - Published by www.plantphysiol.org
Copyright © 2017 American Society of Plant Biologists. All rights reserved.

Pubmed: Author and Title
CrossRef: Author and Title
Google Scholar: Author Only Title Only Author and Title

Paradis E, Claude J, Strimmer K (2004) APE: analyses of phylogenetics and evolution in R language. Bioinformatics 20: 289-290
Pubmed: Author and Title
CrossRef: Author and Title
Google Scholar: Author Only Title Only Author and Title

Rolland-Lagan AG, Prusinkiewicz P (2005) Reviewing models of auxin canalization in the context of leaf vein pattern formation in Arabidopsis. Plant J 44: 854-865
Pubmed: Author and Title
CrossRef: Author and Title
Google Scholar: Author Only Title Only Author and Title

Sachs T (1981) The control of the patterned differentiation of vascular tissue. Adv Bot Res 9: 151-262
Pubmed: Author and Title
CrossRef: Author and Title
Google Scholar: Author Only Title Only Author and Title

Sack L, Cowan PD, Jaikumar N, Holbrook NM (2003) The 'hydrology' of leaves: co-ordination of structure and function in temperate woody species. Plant Cell Environ 26: 1343-1356
Pubmed: Author and Title
CrossRef: Author and Title
Google Scholar: Author Only Title Only Author and Title

Sack L, Frole K (2006) Leaf structural diversity is related to hydraulic capacity in tropical rain forest trees. Ecology 87: 483-491
Pubmed: Author and Title
CrossRef: Author and Title
Google Scholar: Author Only Title Only Author and Title

Sack L, Scoffoni C (2013) Leaf venation: structure, function, development, evolution, ecology and applications in the past, present and future. New Phytol 198: 983-1000
Pubmed: Author and Title
CrossRef: Author and Title
Google Scholar: Author Only Title Only Author and Title

Sack L, Scoffoni C, John GP, Poorter H, Mason CM, Mendez-Alonzo R, Donovan LA (2013) How do leaf veins influence the worldwide leaf economic spectrum? Review and synthesis. J Exp Bot 64: 4053-4080
Pubmed: Author and Title
CrossRef: Author and Title
Google Scholar: Author Only Title Only Author and Title

Scarpella E, Meijer AH (2004) Pattern formation in the vascular system of monocot and dicot plant species. New Phytol 164: 209-242
Pubmed: Author and Title
CrossRef: Author and Title
Google Scholar: Author Only Title Only Author and Title

Schliep KP (2011) phangorn: phylogenetic analysis in R. Bioinformatics 27: 592-593
Pubmed: Author and Title
CrossRef: Author and Title
Google Scholar: Author Only Title Only Author and Title

Scoffoni C, Chatelet DS, Pasquet-kok J, Rawls M, Donoghue MJ, Edwards EJ, Sack L (2016) Hydraulic basis for the evolution of photosynthetic productivity. Nat Plants 2: 16072
Pubmed: Author and Title
CrossRef: Author and Title
Google Scholar: Author Only Title Only Author and Title

Scoffoni C, Kunkle J, Pasquet-Kok J, Vuong C, Patel AJ, Montgomery RA, Givnish TJ, Sack L (2015) Light-induced plasticity in leaf hydraulics, venation, anatomy, and gas exchange in ecologically diverse Hawaiian lobeliads. New Phytol 207: 43-58
Pubmed: Author and Title
CrossRef: Author and Title
Google Scholar: Author Only Title Only Author and Title

Scoffoni C, Rawls M, McKown A, Cochard H, Sack L (2011) Decline of leaf hydraulic conductance with dehydration: relationship to leaf size and venation architecture. Plant Physiol 156: 832-843
Pubmed: Author and Title
CrossRef: Author and Title
Google Scholar: Author Only Title Only Author and Title

Sievers F, Wilm A, Dineen D, Gibson TJ, Karplus K, Li W, Lopez R, McWilliam H, Remmert M, Söding J, Thompson JD, Higgins DG (2011) Fast, scalable generation of high-quality protein multiple sequence alignments using Clustal Omega. Mol Sys Biol 7
Pubmed: Author and Title
CrossRef: Author and Title
Google Scholar: Author Only Title Only Author and Title

Swiecicki WK (1989) A new gene CRISPOID (crd) on chromosome 1. Pisum Newsletter 21: 73-74
Pubmed: Author and Title
CrossRef: Author and Title
Google Scholar: Author Only Title Only Author and Title

Downloaded from on August 3, 2017 - Published by www.plantphysiol.org
Copyright © 2017 American Society of Plant Biologists. All rights reserved.

Tao Y, Ferrer J-L, Ljung K, Pojer F, Hong F, Long JA, Li L, Moreno JE, Bowman ME, Ivans LJ, Cheng Y, Lim J, Zhao Y, Ballaré CL, Sandberg G, Noel JP, Chory J (2008) Rapid synthesis of auxin via a new tryptophan-dependent pathway is required for shade avoidance in plants. Cell 133: 164-176
Pubmed: Author and Title
CrossRef: Author and Title
Google Scholar: Author Only Title Only Author and Title

Tayeh N, Aluome C, Falque M, Jacquin F, Klein A, Chauveau A, Bérard A, Houtin H, Rond C, Kreplak J, Boucherot K, Martin C, Baranger A, Pilet-Nayel M-L, Warkentin TD, Brunel D, Marget P, Le Paslier M-C, Aubert G, Burstin J (2015) Development of two major resources for pea genomics: the GenoPea 13.2K SNP Array and a high-density, high-resolution consensus genetic map. Plant J 84: 1257-1273
Pubmed: Author and Title
CrossRef: Author and Title
Google Scholar: Author Only Title Only Author and Title

Tivendale ND, Davies NW, Molesworth PP, Davidson SE, Smith JA, Lowe EK, Reid JB, Ross JJ (2010) Reassessing the role of N-Hydroxytryptamine in auxin biosynthesis. Plant Physiol 154: 1957-1965
Pubmed: Author and Title
CrossRef: Author and Title
Google Scholar: Author Only Title Only Author and Title

Tobeña-Santamaria R, Bliek M, Ljung K, Sandberg G, Mol JNM, Souer E, Koes R (2002) FLOOZY of petunia is a flavin mono-oxygenase-like protein required for the specification of leaf and flower architecture. Genes Dev 16: 753-763
Pubmed: Author and Title
CrossRef: Author and Title
Google Scholar: Author Only Title Only Author and Title

Tyree MT, Zimmermann MH (2002) Xylem structure and the ascent of sap. Springer, Berlin
Pubmed: Author and Title
CrossRef: Author and Title
Google Scholar: Author Only Title Only Author and Title

Verna C, Sawchuk MG, Linh NM, Scarpella E (2015) Control of vein network topology by auxin transport. BMC Biol 13: 1-16
Pubmed: Author and Title
CrossRef: Author and Title
Google Scholar: Author Only Title Only Author and Title

Wong SC, Cowan IR, Farquhar GD (1979) Stomatal conductance correlates with photosynthetic capacity. Nature 282: 424-426
Pubmed: Author and Title
CrossRef: Author and Title
Google Scholar: Author Only Title Only Author and Title

Yu G, Smith DK, Zhu H, Guan Y, Lam TT-Y (2017) ggtree: an R package for visualization and annotation of phylogenetic trees with their covariates and other associated data. Methods in Ecology and Evolution 8: 28-36
Pubmed: Author and Title
CrossRef: Author and Title
Google Scholar: Author Only Title Only Author and Title

Zhang J, Lin JE, Harris C, Campos Mastrotti Pereira F, Wu F, Blakeslee JJ, Peer WA (2016) DAO1 catalyzes temporal and tissue-specific oxidative inactivation of auxin in Arabidopsis thaliana. Proc Natl Acad Sci USA
Pubmed: Author and Title
CrossRef: Author and Title
Google Scholar: Author Only Title Only Author and Title

Zhang S-B, Sun M, Cao K-F, Hu H, Zhang J-L (2014) Leaf photosynthetic rate of tropical ferns is evolutionarily linked to water transport capacity. PLoS ONE 9: e84682
Pubmed: Author and Title
CrossRef: Author and Title
Google Scholar: Author Only Title Only Author and Title

Zhao Y (2012) Auxin biosynthesis: a simple two-step pathway converts tryptophan to indole-3-acetic acid in plants. Mol Plant 5: 334-338
Pubmed: Author and Title
CrossRef: Author and Title
Google Scholar: Author Only Title Only Author and Title

Zhao Y, Christensen SK, Fankhauser C, Cashman JR, Cohen JD, Weigel D, Chory J (2001) A Role for Flavin Monooxygenase-Like Enzymes in auxin biosynthesis. Science 291: 306-309
Pubmed: Author and Title
CrossRef: Author and Title
Google Scholar: Author Only Title Only Author and Title

Zsögön A, Alves Negrini AC, Peres LEP, Nguyen HT, Ball MC (2015) A mutation that eliminates bundle sheath extensions reduces leaf hydraulic conductance, stomatal conductance and assimilation rates in tomato (Solanum lycopersicum). New Phytol 205: 618-626
Pubmed: Author and Title
CrossRef: Author and Title
Google Scholar: Author Only Title Only Author and Title

Downloaded from on August 3, 2017 - Published by www.plantphysiol.org
Copyright © 2017 American Society of Plant Biologists. All rights reserved.